

Journal of Materials Chemistry B

Accepted Manuscript



This is an *Accepted Manuscript*, which has been through the Royal Society of Chemistry peer review process and has been accepted for publication.

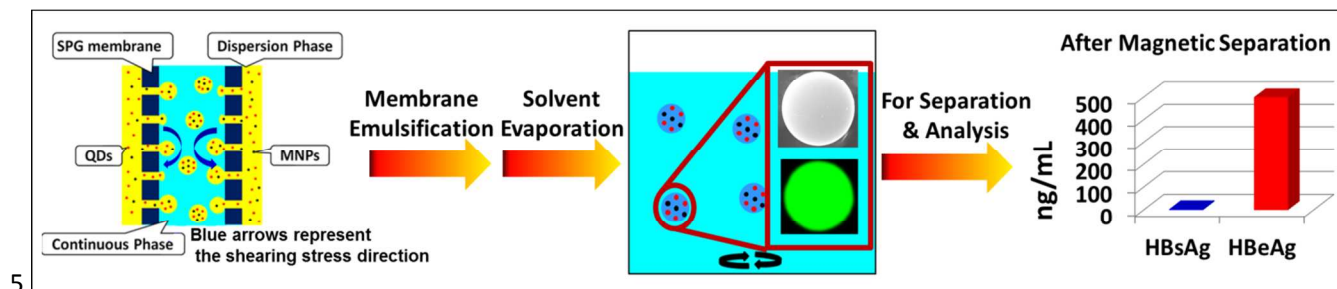
Accepted Manuscripts are published online shortly after acceptance, before technical editing, formatting and proof reading. Using this free service, authors can make their results available to the community, in citable form, before we publish the edited article. We will replace this *Accepted Manuscript* with the edited and formatted *Advance Article* as soon as it is available.

You can find more information about *Accepted Manuscripts* in the [Information for Authors](#).

Please note that technical editing may introduce minor changes to the text and/or graphics, which may alter content. The journal's standard [Terms & Conditions](#) and the [Ethical guidelines](#) still apply. In no event shall the Royal Society of Chemistry be held responsible for any errors or omissions in this *Accepted Manuscript* or any consequences arising from the use of any information it contains.

Graphical Abstract

This communication provides an efficient membrane emulsification-solvent evaporation approach for the preparation of magnetic quantum dot barcodes for ultrasensitive and quantitative bioassays.



Cite this: DOI: 10.1039/c0xx00000x

www.rsc.org/xxxxxx

COMMUNICATION

Efficiently preparation of magnetic quantum dot barcodes

Gang Wang,^{a†} Yuankui Leng,^{a†} Heze Guo,^a Sheng Song,^a Zequan Jiang,^a Xiangliang Yuan,^b Xiebing Wang,^a Kang Sun,^{*a} Kun Sun,^b Hongjing Dou^{*a}

Received (in XXX, XXX) Xth XXXXXXXXX 20XX, Accepted Xth XXXXXXXXX 20XX

DOI: 10.1039/b000000x

Quantum dot (QD)-encoded magnetic barcodes were prepared through a highly efficient membrane emulsification-solvent evaporation approach. Our study demonstrates the great potential of these QD-encoded magnetic barcodes for both magnetic separations and multiplex suspensions assays.

Fluorescent quantum dots (QDs) and superparamagnetic nanoparticles are two important functional inorganic materials which have separately been widely used for numerous biomedical applications.^[1] For example, QDs have been investigated as promising candidates for creating diverse barcodes in suspension assays since these inorganic nanocrystals exhibit narrow emission spectra, high photostability and superior brightness.^[2,3] However, although the suspension assays based on QD-encoded microspheres offer many advantages in disease diagnosis,^[4] they have typically required high sample concentrations and were not effective when only a small amount of dilute sample was available. On the other hand, superparamagnetic nanoparticles such as magnetite nanoparticles (MNPs) have been used to manipulate disease cells and biomolecules for decades,^[5] but they were rarely used in the field of multiplexed biomolecular detection because of the difficulties encountered with encoding the magnetic signatures of microsphere barcodes.^[6] In consideration of the distinct but complementary advantages of QDs and magnetic nanoparticles,^[7] the development of multifunctional composite materials that combine these two nanomaterials together into a micron-sized host microsphere could potentially open new avenues toward ultrasensitive and quantitative bioassays.

Motivated by the great potential value of QD/MNP composite microspheres in bioassays, researchers have explored various approaches to incorporate various magnetic nanoparticles and QDs into microspheres (denoted as MQ-microspheres). These strategies have included the swelling method,^[2d, 8] emulsion polymerization,^[9] layer-by-layer assembly,^[10] and a recently reported concentration-controlled flow focusing (CCFF) technique^[11, 12] developed by Chan *et al.* However, most methods required numerous steps or specialized continuous flow focusing apparatus. The formulation of more efficient approaches that would be required to advance MQ-microspheres production still remains a challenging task.

Herein, we describe a membrane emulsification-solvent evaporation approach (MESE) for embedding both QDs and magnetite nanoparticles within host microspheres in an efficient

manner. Recently, we implemented this MESE approach to fabricate QD-encoded microsphere barcodes.^[13] In this communication, we developed for the first time the MESE approach to fabricate MQ microspheres that possess excellent fluorescent and magnetic properties. Our study demonstrated that both the magnetism and fluorescence of the barcodes could be controlled by adjusting the feed ratio of the MNPs and QDs during the fabrication, and suggested that these MQ microsphere barcodes provide feasible platforms for both hepatitis B virus (HBV) detection and for specific antigen separation.

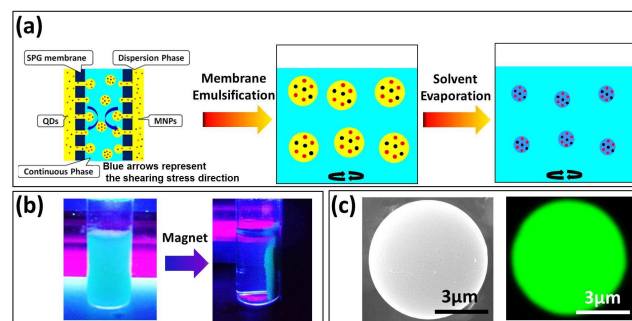


Fig. 1 (a) Schematic diagram depicting the process of fabricating MQ-microspheres *via* the MESE method. (b) Photographs of an aqueous suspension of MQ-microspheres (MQ6) before (left) and after (right) a magnet was placed on the right side of the vial under excitation with a 365 nm UV lamp. (c) SEM (left) and laser confocal fluorescence microscopy (right) images of MQ-microspheres (MQ6).

The combined MESE approach for MQ-microsphere fabrication was performed *via* Shirasu Porous Glass (SPG) membrane emulsification. This route was chosen because SPG membranes could significantly improve the size uniformity of the emulsion droplets and thus that of the resultant microspheres.^[14] As illustrated in Fig. 1a, the organic phase containing QDs, MNPs and poly(styrene-*co*-maleic anhydride) (PSMA) copolymers served as the dispersed phase and was forced by nitrogen pressure through the 4.9 μm SPG membrane pores into the emulsifier-containing aqueous phase. The oil-dispersed QDs and MNPs were synthesized according to methods described in previous reports.^[15] Toluene was used as the oil-phase in this report. Due to the nano-scale sizes and the hydrophobic surfaces of the QDs and MNPs (TEM images are shown in Fig. S1 and Fig. S2 in the Electronic Supplementary Information or ESI), they could readily pass through the SPG membrane and become trapped within the interiors of the emulsion droplets.

Subsequently, the toluene was evaporated from within the droplets and the internal PSMA polymer chains thus became solidified to form microspheres. The diameters of the droplets and thus the sizes of the microspheres could be easily controlled by adjusting the pore size of the membrane. It is noteworthy that this approach provides a significant improvement in the yield. Taking the barcode preparation using a 4.9 μm pore SPG membrane as an example, a droplet generation rate of $\sim 3 \times 10^8$ droplets/mL per hour could be achieved. As disclosed by this study, the resultant MQ-microspheres exhibited good magnetic and fluorescent properties (shown in Fig. 1b), a smooth spherical morphology with a 6.6 μm diameter, a homogeneous QD distribution (shown in Fig. 1c) and a narrow size distribution (see Fig. S3 in the ESI). Moreover, due to the abundant anhydride groups contained within the PSMA matrix, the anhydride groups on the surfaces of the MQ-microspheres could be readily converted to carboxyl groups (see Fig. S4 in the ESI) so that they could be further functionalized with bio-probes *via* acid-catalysed hydrolysis.

As noted earlier, the fluorescent and magnetic properties of the MQ-microspheres could be controlled by adjusting the amount of MNPs and QDs used in the MQ-microsphere fabrication. To evaluate this effect, six families of MQ-microspheres were fabricated through the same procedure but with different feed ratios between the QDs and the MNPs (see the description and Table S1 in the ESI). The laser scanning confocal microscopy (LSCM) images recorded at different focalized planes from the top of the MQ-microspheres to the bottom of the spheres are shown in Fig. 2. By comparing the fluorescence intensities of the four microspheres that contained the same QD content but decreasing MNP contents, (*i.e.*, MQ1, MQ2, MQ3 and MQ4 microspheres as shown in Fig. 2g), it is apparent that the fluorescence intensities of the MQ-microspheres decreased if their MNP content was increased. This may be due to some of the light from the exciting laser and the fluorescence emissions of the QDs being absorbed by the MNPs embedded within the spheres.^[24, 81] This deduction was confirmed by the measurement of the UV-vis absorption spectrum of the MNPs (see Fig. S5 in the ESI), which demonstrated that the MNPs absorbed light up to ~ 700 nm, and thus were capable of absorbing light from both the exciting laser (at 400 nm) and that emitted by the 520 nm QDs. On the other hand, the comparison of the fluorescence intensities of MQ2, MQ4, and MQ5 revealed that the fluorescence intensities of the MQ-microspheres increased if they contained more QDs (see Fig. 2h). In addition, the magnetic properties of the microspheres were studied and the magnetic hysteresis of the MQ-microspheres shown in Fig. 2i indicated that the magnetic properties were related only to the amount of the MNPs, but not to the amount of QDs present within the microspheres.

As a versatile approach for detecting both spectroscopic and size signatures, flow cytometry was established as an effective technique for detecting multiplexed assays. There are two essential requirements for QD-encoded barcodes to be detectable *via* flow cytometry. Specifically, they must emit light within the detection channels of the flow cytometer, and they must exhibit a distinguishable barcode in the flow cytometric histograms. On this basis, our recent study indicated that the 520 and 680 nm

barcodes were both suitable for preparing a flow cytometry-based barcode library.^[13] By utilizing the fluorescence signatures of the barcodes, a two-dimensional barcode library combining the signals of the FL1 (515 \pm 15 nm) and the FL4 (675 \pm 15 nm) channels could be established *via* flow cytometry. Based on this concept, a two-parameter scatter plot was obtained (Figure 3), in which the four dots represented the signals from the two 520 nm MQ-microspheres with different fluorescence intensities (*i.e.*, MQ4 and MQ6), and the two QD-encoded microspheres (*i.e.*, 680 nm Q1 and 520 nm Q2 in which no MNPs were contained).

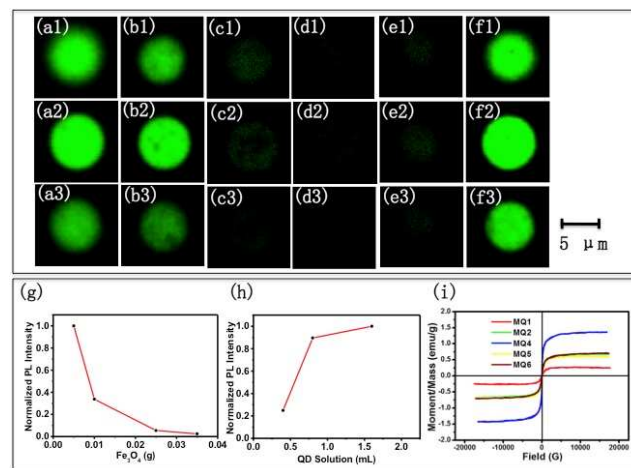


Fig. 2 Images (a1)-(a3), (b1)-(b3), (c1)-(c3), (d1)-(d3), (e1)-(e3) and (f1)-(f3) show LSCM images recorded at three focalized planes from the top to the bottom of MQ1, MQ2, MQ3, MQ4, MQ5 and MQ6 microspheres, respectively. These MQ microspheres were all encoded with 520 nm QDs. (g) The relationship between the fluorescence intensities of the MQ-microspheres and the amount of MNPs added, when the amount of 520 nm QDs was fixed. (h) The relationship between the fluorescence intensity of the MQ-microspheres and the amount of 520 nm QDs added, when the amount of MNPs was fixed. (i) The magnetic hysteresis of MQ1, MQ2, MQ4, MQ5 and MQ6.

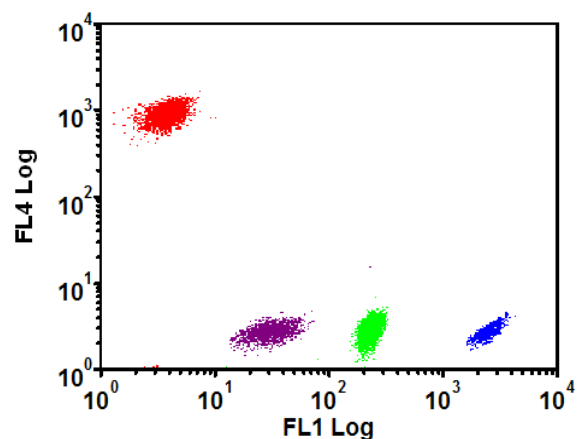


Fig. 3 Plot of log FL4 versus log FL1 for the QD-encoded fluorescent barcodes as obtained *via* flow cytometry.

In the present work, MQ-microspheres and QD-microspheres were used as host vehicles for magnetic separations and immunoassay analysis barcodes, respectively. The hepatitis B surface antigen (HBsAg) and the hepatitis B e antigen (HBeAg), which are both primary indices for HBV diagnosis, were thus

chosen as targets for further immunoassay investigations. As shown in Figure 4a, hepatitis B surface antibodies (HBsAb) and hepatitis B e antibodies (HBeAb) were conjugated onto the surfaces of the microspheres to allow the capture of HBsAg and HBeAg, respectively. MQ6 microspheres were coated with HBsAb probes to achieve a specific magnetic separation of HBsAg from the sample containing 500 ng/mL of HBsAg and 500 ng/mL of HBeAg. To confirm the complete separation of the HBsAg, the HBsAb-coated Q1 microspheres and HBeAb-coated Q2 microspheres were added into the sample for further multiplex suspension bioassay measurements. As shown in Figure 4b, the residual antigens in the sample could be captured via their conjugation with the antibody probes on the microsphere surfaces. Subsequently, biotin-HBsAb, biotin-HBeAb, and the fluorescent probe phycoerythrin (PE) were added to form sandwich immunoassay structures on the surfaces of the microspheres. The concentrations of the target molecules in the samples corresponded closely with the median fluorescence intensities (MFI) of the labelled PE reporters. The concentration of residual HBsAg in the sample was calculated quantitatively based on a pre-established MFI-HBsAg calibration curve (see Fig. S6 in the ESI), and the results are summarized in Figure 4c. The HBsAg concentration decreased sharply from 500 to 3 ng/mL after the magnetic separation had been performed, whereas the concentration of HBeAg still remained constant. This behaviour indicated that the MQ-microspheres were effective in providing specific magnetic separation, and a QD-microsphere based multiplex suspension assay can be used further to evaluate the effectiveness of the separation with high sensitivity.

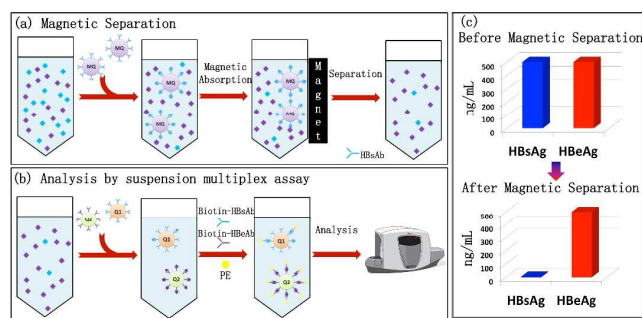


Fig. 4 Schematic diagram depicting (a) the magnetic separation of HBsAg with MQ-microspheres and (b) a multiplex suspension assay utilizing QD-microspheres. (c) displays the change on the concentration of HBsAg and HBeAg in sample after MQ-microspheres based magnetic separation. The blue and purple blocks in (a) and (b) represent HBsAg and HBeAg, respectively.

In summary, a MESE method was developed to efficiently fabricate MQ-microspheres. The magnetic and fluorescent properties of the microspheres could be readily controlled by adjusting the amount of nanoparticles employed in the fabrication. Investigations on the effectiveness of these MQ-microspheres in targeting HBsAg and HBeAg in immunoassays demonstrated that these MQ-microspheres have great potential as hosts for magnetic separations and as probes for the analysis of biomolecules.

Acknowledgements

Prof. H. Dou thanks the financial support of the National Natural Science Foundation of China (Nos. 21174082, 21374061), the

SJTU SMC-Chen Xing Young Scholars Award, Program of New Century Excellent Talent in University (NCET-13-0360), International Science and Technology Cooperation Project of the Science and Technology Commission of Shanghai Municipality (No. 14520710300) and the Instrumental Analysis Center of the SJTU.

Notes and References

[†] These two authors contributed equally.

^a The State Key Laboratory of Metal Matrix Composites, School of Materials Science and Engineering, Shanghai Jiao Tong University, Shanghai 200240, P. R. China, E-mail: hjdou@sjtu.edu.cn (H. Dou); ksun@sjtu.edu.cn (K. Sun)

^b Xin Hua Hospital, School of Medicine, Shanghai Jiao Tong University, Shanghai, 200092, P. R. China P. R. China

Electronic Supplementary Information (ESI) available: Experimental details. See DOI: 10.1039/b000000x/

- [1] a) J. Hu, C. Y. Wen, Z. L. Zhang, M. Xie, M. Wu and D. W. Pang, *Anal. Chem.* 2013, **85**, 11929-11935; b) Y. H. Chan, Y. H. Jin, C. F. Wu and D. T. Chiu, *Chem. Commun.* 2011, **47**, 2820-2822; c) Q. Tian, W. N. Wong, Y. Xu, Y. T. Chan, H. K. Ho, G. Pastorin and W. H. Ang, *Chem. Commun.* 2012, **48**, 5467-5469.
- [2] a) C. T. Lim and Y. Zhang, *Biosens. Bioelectron.* 2007, **22**, 1197-1204; b) H. Kuramitz, *Anal. Bioanal. Chem.* 2009, **394**, 61-69; c) R. Wilson, A. R. Cossins and D. G. Spiller, *Angew. Chem. Int. Ed.* 2006, **45**, 6104-6117; d) Y.-H. Li, T. Song, J.-Q. Liu, S.-J. Zhu and J. Chang, *J. Mater. Chem.* 2011, **21**, 12520.
- [3] S. Birtwell and H. Morgan, *Integr. Biol.* 2009, **1**, 345.
- [4] a) S. Nie, M. Y. Han, X. H. Gao and J. Z. Su, *Nat. Biotechnol.* 2001, **19**, 631-635; b) S. Fournier - Bidoz, T. L. Jennings, J. M. Klostranec, W. Fung, A. Rhee, D. Li and W. C. W. Chan, *Angew. Chem. Int. Ed.* 2008, **47**, 5577-5581; c) R. Gill, M. Zayats and I. Willner, *Angew. Chem. Int. Ed.* 2008, **47**, 7602-7625.
- [5] a) N. Ahmed, H. Fessi and A. Elaissari, *Drug Discovery Today* 2012, **17**, 928-934; b) R. Banerjee, Y. Katsenovich, L. Lagos, M. McIntosh, X. Zhang and C. Z. Li, *Curr. Med. Chem.* 2010, **17**, 3120-3141.
- [6] a) I. Jeong, Y. J. Eu, K. W. Kim, X. H. Hu, B. Sinha and C. Kim, *Journal of Magnetism* 2012, **17**, 302-307; b) Y. K. Hahn, Z. Jin, J. H. Kang, E. Oh, M. K. Han, H. S. Kim, J. T. Jang, J. H. Lee, J. Cheon, S. H. Kim, H. S. Park and J. K. Park, *Anal. Chem.* 2007, **79**, 2214-2220.
- [7] a) X. Zhu, D. Duan and N. G. Publicover, *The Analyst* 2010, **135**, 381; b) L. Zhang, H. Xue, Z. Cao, A. Keefe, J. Wang and S. Jiang, *Biomaterials* 2011, **32**, 4604-4608.
- [8] T. R. Sathe, A. Agrawal and S. Nie, *Anal. Chem.* 2006, **78**, 5627-5632.
- [9] a) Y. Yang, C. Tu and M. Gao, *J. Mater. Chem.* 2007, **17**, 2930; b) C. Tu, Y. Yang and M. Gao, *Nanotechnology* 2008, **19**, 105601; c) Y. J. Zhao, H. C. Shum, H. S. Chen, L. L. A. Adams, Z. Z. Gu and D. A. Weitz, *J. Am. Chem. Soc.* 2011, **133**, 8790-8793.
- [10] a) H. Wang, L. Sun, Y. Li, X. Fei, M. Sun, C. Zhang, Y. Li and Q. Yang, *Langmuir* 2001, **27**, 11609-11615; b) S. Rauf, A. Glidle and J. M. Cooper, *Chem. Commun.* 2010, **46**, 2814; c) Q. B. Wang, Y. Liu, C. X. Lin and H. Yan, *Nanotechnology* 2007, **18**, 405604.
- [11] S. Giri, D. W. Li and W. C. W. Chan, *Chem. Commun.* 2011,

47, 4195-4197.

[12] K. K. Jain, *Exp. Rev. Mol. Diagn.* 2003, **3**, 153-161.

[13] G. Wang, Y. K. Leng, H. J. Dou, L. Wang, W. W. Li, X. B. Wang, K. Sun, L. S. Shen, X. L. Yuan, J. Y. Li, J. S. Han, H. S.

5 Xiao and Y. Li, *ACS Nano* 2013, **7**, 471-481.

[14] a) S. M. Joscelyne and G. Trägårdh, *J. Membrane Sci.* 2000, **169**, 107-117; b) S. Omi, G. Ma and M. Nagai, *Macromol. Symp.* 2000, **151**, 319-330.

[15] a) J. Park, K. An, Y. Hwang, J.-G. Park, H.-J. Noh, J.-Y.
10 Kim, J.-H. Park, N.-M. Hwang and T. Hyeon, *Nat. Mater.* 2004, **3**, 891-895; b) X. Wang, W. Li and K. Sun, *J. Mater. Chem.* 2011, **21**, 8558-8565; c) B. Xing, W. Li, X. Wang, H. Dou, L. Wang, K. Sun, X. He, J. Han, H. Xiao, J. Miao and Y. Li, *J. Mater. Chem.* 2010, **20**, 5664.